Implications of Jovian X-ray emission for magnetosphere-ionosphere coupling

T. E. Cravens,[1] J. H. Waite,[2] T. I. Gombosi,[2] N. Lugaz,[2] G. R. Gladstone,[3] B. H. Mauk,[4] and R. J. MacDowall[5]

Received 19 May 2003; revised 20 October 2003; accepted 23 October 2003; published 31 December 2003.

[1] The first observations of Jupiter made by the Chandra X-Ray Observatory revealed a powerful X-ray aurora located in the polar caps. The X-ray emission exhibited a 40-min periodicity. Such 40-min periodicities have previously been seen in energetic particle fluxes and in Jovian radio emission. This paper develops scenarios in which the X-ray emission is produced by energetic heavy ion precipitation, either on open field lines connecting to the solar wind or on closed field lines reaching to the outer magnetosphere. In order to produce enough X-ray power, both scenarios require the existence of field-aligned electric fields located somewhere between the ionosphere and the magnetosphere, most likely at a radial distance of a few Jovian radii. The potential needed for solar wind ions to produce the observed X-rays is about 200 kV and the potential needed for the magnetospheric ions is at least 8 MV. Protons and helium ions are also accelerated by the potential and should produce an intense ultraviolet aurora. Downward electrical current is carried by the precipitating ions and also by upwardly accelerated secondary electrons produced by the primary ion precipitation. The estimated downward Birkeland current is about 1000 MA for the solar wind case and is about 10 MA for the magnetospheric case. For the magnetosphere scenario, this observed current represents part of the "return" current portion of the magnetospheric circuit associated with the departure of the mass-loaded magnetospheric plasma from corotation. The auroral X-ray emission maps at least part of this return current in the polar cap, whereas the main oval, produced by electron precipitation, is thought to map the region of upward Birkeland currents. The accelerated secondary electrons could be responsible for the periodic radio emission (i.e., QP-40 bursts). *INDEX TERMS:* 2736 Magnetospheric Physics: Magnetosphere/ionosphere interactions; 2455 Ionosphere: Particle precipitation; 2704 Magnetospheric Physics: Auroral phenomena (2407); 2756 Magnetospheric Physics: Planetary magnetospheres (5443, 5737, 6030); *KEYWORDS:* planetary magnetospheres, Jovian aurora, Jovian magnetosphere, X-rays, ion acceleration, field-aligned currents

Citation: Cravens, T. E., J. H. Waite, T. I. Gombosi, N. Lugaz, G. R. Gladstone, B. H. Mauk, and R. J. MacDowall, Implications of Jovian X-ray emission for magnetosphere-ionosphere coupling, *J. Geophys. Res.*, *108*(A12), 1465, doi:10.1029/2003JA010050, 2003.

1. Introduction

[2] Jupiter is known to have a powerful aurora [cf., *Waite and Lummerzheim*, 2002] with a total power in the range of $10^{13}-10^{14}$ W. Auroral emission has been observed throughout the electromagnetic spectrum (visible, ultraviolet, infrared, and X-ray) [cf., *Bhardwaj and Gladstone*, 2000]. The most intense emission comes in the ultraviolet part of the spectrum from the Lyman and Werner bands of H_2 and Lyman alpha emission from atomic hydrogen. Jovian x-ray emission was first observed in 1979 with the Einstein Observatory [*Metzger et al.*, 1983] but has also been observed with the Roentgen satellite (ROSAT) [e.g., *Waite et al.*, 1994] and with the Chandra X-Ray Observatory (CXO) [*Gladstone et al.*, 2002]. The auroral X-ray power deduced from these observations is about 10^9 W.

[3] The spectral resolution of the ROSAT X-ray observations [e.g., *Metzger et al.*, 1983; *Waite et al.*, 1994] was sufficient to indicate that the X-ray emission was "soft," with photon energies between about 0.1 and 1 keV, but not good enough to clearly distinguish between a continuum source (i.e., bremsstrahlung) and a line-emission source, although the lines explanation did seem to provide a better spectral fit [*Metzger et al.*, 1983; *Waite et al.*, 1994; *Cravens et al.*, 1995]. *Metzger et al.* [1983] suggested that energetic heavy sulfur and oxygen ion precipitation was responsible for the Jovian X-ray emission seen by the Einstein observatory. Analysis of heavy ion fluxes measured by the

[1]Department of Physics and Astronomy, University of Kansas, Lawrence, Kansas, USA.
[2]Space Physics Research Laboratory, University of Michigan, Ann Arbor, Michigan, USA.
[3]Southwest Research Institute, San Antonio, Texas, USA.
[4]The Johns Hopkins University, Applied Physics Laboratory, Laurel, Maryland, USA.
[5]NASA Goddard Space Flight Center, Greenbelt, Maryland, USA.

0148-0227/03/2003JA010050

Voyager spacecraft at radial distances of about 10–20 Jovian radii (R_J) in the Jovian magnetosphere suggested that such ions might indeed precipitate into the atmosphere [*Gehrels and Stone*, 1983].

[4] On the other hand, *Barbosa* [1992] proposed that bremsstrahlung emission associated with energetic electron precipitation was responsible for Jovian X-ray emission. In favor of this mechanism is the fact that X-rays are known to be produced by bremsstrahlung in the terrestrial aurora by energetic electrons, although the X-rays are more energetic than the soft X-rays (energies less than 1 keV) observed from Jupiter. *Metzger et al.* [1983] and *Waite et al.* [1992] demonstrated that to produce 1 GW of X-ray power with bremsstrahlung a total auroral power in excess of 10^{15} W is required, which far exceeds the 10^{13}–10^{14} W auroral power suggested by the UV measurements.

[5] Detailed calculations by *Cravens et al.* [1995], *Kharchenko et al.* [1998], and *Liu and Schultz* [1999, 2000] indicated that precipitation of S and O ions with energies in excess of 0.5 MeV/amu, and consistent with the Gehrels and Stone spectrum, could indeed reproduce the X-ray observations. It was shown that the observed soft X-ray power of 1 GW could be generated with a total power input in heavy ions of only $\approx 10^{12}$ W. Most of the X-ray emission is produced by transitions taking place in highly charged ions (e.g., O^{6+} and O^{7+}) produced by electron removal collisions during the precipitation process.

[6] The popular view then, until very recently, was that most of the observed UV emission comes from energetic electrons (mostly above, or near the top of, the homopause, below which UV-absorbing methane resides), whereas the X-ray emission was produced by energetic heavy ion precipitation from the middle magnetosphere. However, recent high spatial resolution observations carried out by CXO have altered at least some of our suppositions about the X-ray aurora. The observed X-ray emission [*Gladstone et al.*, 2002] has two distinct components: (1) emission spread uniformly over the disk (including low and middle latitudes), and (2) auroral emission which is spatially very localized in the polar cap at latitudes higher than the main auroral oval. Each of these components has an emitted power of about 1 GW. Most of the auroral emission originates from a rather small area (10^{13} to 10^{14} m^2) with intensities that are typically about 2–20 R [*Gladstone et al.*, 2002]. Note that 1 R, or Rayleigh, is a unit of 4πI given by 10^6 cm^{-2} s^{-1} (or 10^{10} m^{-2} s^{-1}), where the intensity, I, has units of cm^{-2} s^{-1} sr^{-1} (or m^{-2} s^{-1} sr^{-1}). The disk emission can probably be largely explained by the atmospheric scattering of solar X-rays [*Maurellis et al.*, 2000; *Cravens and Maurellis*, 2001]. The X-rays observed by CXO [*Gladstone et al.*, 2002] are also soft X-rays with energies in the 100 eV to 1 keV range. The CXO HRC energy range is 0.1–2. keV with a peak near 1.1 keV [*Gladstone et al.*, 2002], but the ROSAT observations place the photon energies mainly below 1 keV.

[7] The auroral emission has another interesting characteristic; it has a strong periodic component with a period of about 40 min. Energetic ion and electron fluxes in the Jovian magnetosphere, and even outside the magnetosphere, also exhibit 40 min periodicities at times [*Simpson et al.*, 1992; *McKibben et al.*, 1993; *Anagnostopoulos et al.*, 1998; *Marhavilas et al.*, 2001]. And 40-min periodicities have been observed in a type of radio emission detected from Jupiter and called quasi-periodic bursts (i.e., QP-40 bursts) [*MacDowall et al.*, 1993], although a range of periodicities (e.g., 25–30 min.) have also been observed. This QP emission is thought to be cyclotron maser instability emission originating from accelerated electrons with a source location a few R_J above the auroral region [*MacDowall et al.*, 1993]. Somehow, the energetic ions, electrons, and radio emission are linked with the X-ray emission.

[8] The main auroral oval as observed in the UV (mainly H_2 Lyman and Werner band emission) by the Hubble Space Telescope (HST) or other UV telescopes [*Clarke et al.*, 1998; *Gérard et al.*, 1993; *Prangé et al.*, 1998; cf. *Bhardwaj and Gladstone*, 2000; *Waite and Lummerzheim*, 2002; *Galand and Chakrabarti*, 2002] is confined to a narrow-latitude band mapping to a radial distance in the magnetosphere of about 30 R_J. Some polar cap UV emission has also been observed, including some ''flare-like'' emission [*Bhardwaj and Gladstone*, 2000]. The auroral X-ray emission observed by CXO must map, then, to radial distances significantly higher than 30 R_J, that is, to the outer magnetosphere, or possibly even to open field lines connecting to the interplanetary magnetic field. Consequently, energetic heavy ion populations observed in the middle magnetosphere [i.e., *Gehrels and Stone*, 1983] can no longer be invoked as an explanation for the X-ray aurora.

[9] The purpose of the current paper is to explore how soft X-ray emission can be produced in the polar cap and to explore the magnetospheric implications of this emission. Two scenarios seem possible: (1) highly charged solar wind heavy ions enter the magnetospheric cusp (on open field lines), are accelerated by a field-aligned potential, and then precipitate into the polar cap; (2) heavy (e.g., S and O) ions in the outer magnetosphere (on closed field lines) are accelerated by a field-aligned potential and precipitate. In the first case, the solar wind heavy ions are already in high charge states (reflecting their origin in the solar corona) and produce X-rays due to charge transfer collisions leading to highly excited product ions. The mechanism in this case is essentially the same as the solar wind charge exchange method (SWCX), which has been used to explain cometary X-ray emission (see the review by *Cravens* [2002] for a discussion of both observations and theory). In the second case, high charge state sulfur and oxygen ions produce X-rays via charge exchange collisions (and perhaps by direct excitation also). However, the original magnetospheric ions are not present in high enough charge states to produce X-rays so that further acceleration by a parallel electric field is needed. The parallel electric field also enhances the ion flux. It has been shown that to obtain excited O^{6+} or O^{7+} type ions via the precipitation process, the original ion energy must be about 1 MeV/amu or greater [*Cravens et al.*, 1995]. This scenario is similar to the original middle magnetosphere heavy ion scenario but with the extra ingredient of a large field-aligned potential (and at a different location).

[10] For both the solar wind ion and magnetospheric ion scenarios, protons and alpha particles are also accelerated by the parallel electric field and precipitate into the atmosphere. All these ions carry electrical current, as do upwardly accelerated secondary electrons produced by the auroral precipitation. We demonstrate in this paper that the downward field-aligned electrical current (i.e., a Birke-

land current) into the polar cap is in excess of several MA. As mentioned above, in this paper, the term polar cap will refer to all latitudes poleward of the main auroral oval regardless of whether or not the field lines are open or closed. For the solar wind scenario the field lines are open, and for the magnetospheric ion scenario the field lines are closed.

[11] *Mauk et al.* [2002] reviewed magnetosphere-ionosphere coupling at both Earth and Jupiter and put auroral precipitation into the context of magnetospheric dynamics. An extensive discussion (and lists of references) on the electrical current system in Jupiter's magnetosphere, including field-aligned currents, can be found in the introductory sections of *Hill* [2001] and *Cowley et al.* [2003]. A magnetospheric current system associated with the partial corotation of magnetospheric plasma at Jupiter was suggested by *Hill* [1979] and by *Vasyliunas* [1983]. More recently, the main oval ultraviolet emissions have been linked to currents originating in the middle magnetosphere [*Barbosa*, 1984; *Gérard et al.*, 1994; *Dougherty et al.*, 1993; *Cowley et al.*, 1996] (see *Cowley et al.* [2003] for a more complete discussion of this literature). Field-aligned currents (into the ionosphere) estimated from magnetic field measurements in the middle magnetosphere [*Bunce and Cowley*, 2001; *Khurana*, 2001; *Bunce et al.*, 2002] are rather large at about $0.1-1$ μA m^{-2}. The total upward current for the partial corotation current system is about 100 MA [*Cowley et al.*, 2003]. It has further been suggested that such upward currents require the existence of field-aligned potentials of about 100 kV which accelerate electrons downward into the main auroral oval [*Hill*, 2001; *Bunce and Cowley*, 2001; *Cowley and Bunce*, 2001; *Cowley et al.*, 2003].

[12] *Hill* [2001] developed a theoretical model linking these currents to the dynamics such that the currents enforce the partial corotation of the outwardly moving magnetospheric plasma. This model, which assumed a dipole magnetic field, explains why the maximum upward current density occurs near a radial distance of $\approx$30 R_J. A total current of about 10–30 MA was obtained. A similar approach but including nondipole magnetic field effects gave total currents more like 100 MA [*Cowley and Bunce*, 2001; *Cowley et al.*, 2003]. This scenario necessitates the existence of downward "return" currents at latitudes higher than the main oval (i.e., radial distances beyond 30 R_J). Figure 1 is a schematic illustrating this current system and the locations of particle populations possibly responsible for the auroral X-ray emission. For the scenario in this paper, in which magnetospheric ions cause the X-ray emission, this emission might act as a diagnostic for at least some of the return current in this Jovian current system. On the other hand, for the case in which solar wind ions on open magnetic field lines produce the X-ray emission, the currents carried by the ions are part of some other current system linking to the magnetosheath plasma (system 1 Birkeland currents in terrestrial magnetosphere terminology).

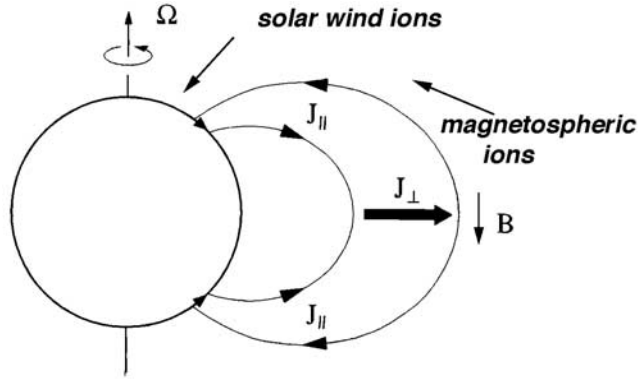

Figure 1. Schematic of the Jovian magnetosphere showing electrical current system relevant to the auroral precipitation discussed in this paper. The schematic is not to scale; the size of Jupiter is greatly exaggerated and the field lines at large radial distances are actually distorted outwards [e.g., see *Engle and Beard*, 1980]. The upward field-aligned currents connect to the main auroral oval and go out to the middle magnetosphere (distances of about 30–50 R_J) whereas the downward return current comes from the outer magnetosphere (50–100 R_J) down to latitudes on Jupiter poleward of the main auroral oval (called the polar cap in the text). Also shown are possible locations of the solar wind and magnetospheric ion populations that might be responsible for the auroral X-ray emission. Solar wind ions would enter the magnetosphere in the cusp region on open field lines connecting to the solar wind. In both cases, a field-aligned electric potential is required at a location of a few R_J over the polar caps. Adapted from a schematic in the work of *Hill* [2001].

2. Solar Wind Charge Exchange Mechanism and the Jovian Aurora

[13] X-ray emission from comets was discovered by ROSAT in 1996 [*Lisse et al.*, 1996] and was subsequently explained as being due to charge exchange collisions of high charge state heavy solar wind ions with cometary neutrals [*Cravens*, 1997a] (see review by *Cravens* [2002]). Subsequent observations and modeling work has supported this explanation [cf. *Cravens*, 2002]. For example, the charge transfer reaction for a solar wind O^{7+} ion with a neutral species M (H_2O for comets or H_2 for Jupiter) can be represented by the reaction:

$$O^{7+} + M \rightarrow O^{6+}* + M^{+}, \quad (1)$$

where $O^{6+}*$ is an excited state of the O^{6+} ion and emits at least one X-ray photon. The cross sections for such charge transfer collisions are very high at solar wind energies, exceeding 10^{-15} cm^2 [e.g., *Greenwood et al.*, 2001]. A very large number of lines are produced by this mechanism from a large number of solar wind ion species. Recently, CXO has made high enough spectral resolution observations [*Lisse et al.*, 2001; *Krasnopolsky et al.*, 2002] to reveal the presence in the 0.3 to 1 keV energy range of discrete transitions from O^{7+}, O^{6+}, and probably C^{5+} and Ne^{8+} ion species.

2.1. Nonaccelerated Solar Wind Ions

[14] Let us first apply the SWCX mechanism to Jupiter without additional ion acceleration. Solar wind ions (including high charge state heavy ions) in the magnetosheath [*Geiss et al.*, 1992] should have access to the Jovian

atmosphere in the cusp/cleft region which contains newly opened magnetic field lines. Solar wind plasma is known to penetrate to the atmosphere in the terrestrial cusp [cf. *Reiff et al.*, 1977; *Onsager et al.*, 1993]. The low-altitude polar cusp is typically located near local noon in the polar cap, at least for southward IMF. The ion distribution function in the magnetosheath cusp region is assumed to be roughly isotropic. The particle intensity for such a distribution remains the same along a magnetic field line [*Walt*, 1994]. We thus assume that the particle flux at the top of the atmosphere (in the low-altitude cusp) is just the magnetosheath flux. We assume that the solar wind plasma has "direct" access to the Jovian atmosphere in the cusp region, and with this assumption we then estimate the X-ray flux from the resulting solar wind ion precipitation.

[15] We now estimate the X-ray emission produced by this cusp precipitation. Each solar wind heavy ion that encounters a neutral (i.e., reaches the atmosphere) will quickly charge transfer and produce an X-ray photon. The resulting ion is also a high charge state ion and produces an X-ray or extreme ultraviolet (EUV) photon. The integrated production rate of photons will just be the solar wind heavy ion flux, F, at the top of the atmosphere times a factor, N, of 2 or 3 for the number of photons per ion. The heavy ion flux is the fraction of heavy ions in the solar wind, f, multiplied by the solar wind proton flux where $f \approx 10^{-3}$. The "isotropic" proton flux in the magnetosheath is roughly the upstream proton flux, $n_{sw}u_{sw}$, multiplied by some flank magnetosheath enhancement factor (perhaps about 2) [*Spreiter et al.*, 1966], where n_{sw} is the proton density at 5 AU and $u_{sw} \approx 400$ km/s is the solar wind speed. A very approximate expression for the X-ray intensity emitted from the region of the atmosphere subject to this precipitation is

$$4\pi I \approx 2 n_{sw} u_{sw} f N. \quad (2)$$

The solar wind density at 5 AU is typically about 0.4 cm^{-3}, although it is extremely variable. With these numbers, equation (2) gives $4\pi I \approx 10^5$ cm^{-2} s^{-1} = 0.1 R. The observed value of $4\pi I$ is about 2–20 R [*Gladstone et al.*, 2002]. For an auroral area of $A \approx 10^{14}$ m^2 and for a typical photon energy of ≈300 eV, the total X-ray power (both hemispheres) from the SWCX mechanism is ≈50 MW. The observed power is much higher at about 1 GW (this is equivalent to an intensity of about 2 R, or to an intensity as high as 20 R if a smaller area of 10^{13} m^2 is used). These numbers would be consistent with a global entry rate of roughly 10^{23} heavy ions per second (and 10^{26} s^{-1} for solar wind protons and 10^{25} s^{-1} for alpha particles) into the high-altitude cusp at the magnetopause. It should be noted that little is known about the cusp region of Jupiter and the analysis in this paper was based on an Earth-like cusp. However, the radio experiment onboard Ulysses detected auroral hiss at Jupiter with a radiated power of about 10^7 W and this was interpreted as being associated with a cusp by analogy with terrestrial auroral hiss [*Farrell et al.*, 1993]. A solar wind input of 10^{10}–10^{12} W was estimated using terrestrial efficiencies for this type of radio emission.

2.2. Accelerated Solar Wind Ions

[16] Our SWCX cusp mechanism generates X-ray intensities (or powers) that are a factor of 20 to 200 smaller than the values measured by CXO or ROSAT. One way to boost the flux of solar wind ions at the top of the atmosphere (and hence the X-ray power) is to apply a parallel electric field along the magnetic field line, somewhere between the magnetopause and the atmosphere. As pointed out by *Knight* [1973] and then applied by *Lyons* [1982] to the terrestrial aurora, a field-aligned potential drop can enhance the precipitating flux (for an initially isotropic flux) by effectively enlarging the loss cone. Such field-aligned potentials are thought to be responsible for discrete auroral events (i.e., inverted-V events) at Earth [cf. *Mauk et al.*, 2002]. *Cowley and Bunce* [2001] and *Cowley et al.* [2003] suggested that such potentials are responsible for electron acceleration at the main auroral oval at Jupiter. These potential structures are thought to develop in response to the demands of the magnetospheric "electrical circuit" for a current density that exceeds the maximum current density that can be carried by a thermal distribution of charge carriers (i.e., plasmasheet electrons for terrestrial inverted-V events).

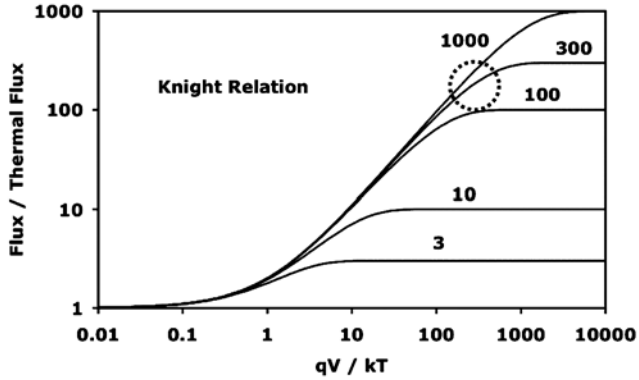

Figure 2. The Knight relation. Parallel particle flux (relative to the thermal flux) versus the parallel potential drop relative to the thermal energy. Each curve is labeled with the magnetic mirror ratio between the ionosphere and the top of the acceleration region. The circle shows the approximate area of the diagram relevant to both the solar wind ion and the magnetospheric ion precipitation scenarios discussed in the paper.

[17] The ratio of the current density to the maximum "thermal" current density can be expressed as a function of the parallel potential and the magnetic mirror ratio between the top of the acceleration region and the ionosphere (i.e., the Knight relation) [*Knight*, 1973; *Lyons*, 1982]. Figure 2 displays the Knight relation for the particle flux for several values of the mirror ratio. The parallel particle flux into the ionosphere is proportional to the field-aligned electrical current into the ionosphere. The ratio of the accelerated flux (F) to the initial thermal flux (F_{th}) is denoted as $R_{knight} = F/F_{th}$. The initial thermal flux is approximately $F_{th} \approx n\, u_{th}$, where the density and thermal speed of the original ambient ion population are n and u_{th}, respectively. The parallel kinetic energy gained by a particle due to the parallel potential drop is $K_{||} = q\, V_{||}$, where q is the charge and $V_{||}$ is the potential drop (units of Volts). One notices from Figure 2 that the flux expression is linear in the variable $K_{||}/K_{th}$ for very large mirror ratios (that is, $R_{knight} \approx K_{||}/K_{th}$).

[18] How does the Knight relation help us produce X-rays at Jupiter? In order to boost the flux of heavy solar wind ions

at the atmosphere, we postulate the existence of a downward potential along magnetic field lines in the cusp/cleft region. From our earlier estimates of the SWCX mechanism we need a boost in the particle flux of a factor of 20 to 200 from unaccelerated fluxes, as discussed earlier, in order to obtain a sufficiently large heavy ion flux to explain the X-ray observations. Hence, we need a "Knight factor" equal to this, and we set R_{knight} equal to ≈100. The magnetic mirror ratio between the magnetopause and the atmosphere exceeds 10^5, but a ratio of ≈100 would suffice to allow a value of $R_{knight} \approx 100$. Hence the location of the potential drop region could be almost anywhere along the field beyond about 5 R_J (Jovian radii). Adopting the approximation of a linear Knight relation, we need $K_{||} \approx R_{knight}\, K_{th} \approx 100\, K_{th}$. For typical solar wind ions in the magnetosheath a reasonable value of the thermal energy is $K_{th} \approx M$ keV, where M is the ion mass in amu (e.g., 1 amu for protons and 16 amu for oxygen ions) and using the fact that the typical kinetic energy of a solar wind ion is 1 keV/amu. Implicit in this K_{th} discussion is that heavy ions in the shocked solar wind of the magnetosheath have the same thermal speed as protons rather than the same temperature [*Geiss et al.*, 1992].

[19] In order to explain the X-ray observations we need the field-aligned potential discussed above to accelerate heavy solar wind ions to total energies of $K_{||} \approx 100\, K_{th} \approx 100$ M keV (equivalent to 100 keV/amu). For oxygen the total energy needed post-acceleration is ≈1.6 MeV. The parallel electrical potential needed to produce this energy is $V_{||} = K_{||}/q = 100\,(M/q)$ keV ≈ $(16/7)\,10^5$ V ≈ 200 kV, for a typical solar wind O^{7+} ion. Highly charged heavy solar wind ions other than O^{7+} will be accelerated to different energies depending on their charge and mass, but we will set the parameters for this paper using oxygen which is the most abundant solar wind heavy ion. Each heavy solar wind ion produces approximately two X-ray photons, independent of its energy, for energies less than about 0.5 MeV/amu [*Cravens et al.*, 1995]. Hence each ion that reaches the atmosphere produces the same number of photons, whether or not this ion was accelerated. However, for ion energies exceeding about 0.5 MeV/amu the electron removal cross section becomes large enough in comparison with the charge transfer cross section such that each incident ion is able to produce more than one or two photons [cf. *Cravens et al.*, 1995]. At the energies relevant to this section of the paper, the parallel electric field enhances the X-ray emission by enhancing the ion flux reaching the atmosphere rather than by increasing the X-ray production efficiency per ion.

[20] By means of the parallel electric field, the flux of heavy solar wind ions into the atmosphere can be sufficiently enhanced to produce the soft X-ray power (or intensity) observed by CXO or ROSAT. However, this potential has other implications. In particular, the proton flux in the solar wind is about 1000 times (i.e., 1/f) greater than the heavy ion flux. The protons (and alpha particles) are also accelerated by the 200 kV potential. The resulting proton flux at the top of the atmosphere is given by:

$$F_{proton} \approx f^{-1} F \approx f^{-1} R_{knight} F_{th} \approx 2\, R_{knight} n_{sw} u_{sw} \approx 10^{10} cm^{-2} s^{-1}. \quad (3)$$

The proton energy flux is (100 keV) × F_{proton} which gives a proton energy flux of ≈1 W m^{-2}. This is a large energy flux in comparison with typical electron energy fluxes adopted for the main auroral oval [e.g., *Grodent et al.*, 2001]. Using an auroral area of A ≈ 10^{14} m^2, the total polar cap auroral power (or luminosity L_{tot}) associated with the accelerated solar wind proton/ion precipitation is $L_{tot} \approx 10^{14}$ W. Such a proton aurora would emit mainly ultraviolet radiation and such a large luminosity should have been observable. Instead, observations indicate that the main oval auroral power usually exceeds that of the polar cap in the ultraviolet [see *Bhardwaj and Gladstone*, 2000]. However, during polar UV "flares" the UV brightness can reach intensities of tens of MR for a minute or so with associated power densities of several W m^{-2} [*Waite et al.*, 2001].

[21] The solar wind ions (mostly protons) also carry a downward Birkeland current of $I_{||} = e\, A\, F_{protons} \approx 10^9$ Amps = 1000 MA. This current connects to the magnetosheath rather than the magnetosphere, but to put its magnitude into context, it is 30 times greater than the *Hill* [2001] estimate for the total magnetospheric circuit and 10 times the *Cowley et al.* [2003] estimate and it still does not include any contribution from electrons caught in the potential and accelerated upward (to 100 keV energies). Even if the adopted auroral area were smaller, at 10^{13} m^2, the current would still be as large as 100 MA and the total associated auroral power would be ≈10^{13} W. Of course, in this case, the X-ray power would be only ≈0.1 GW, which is less than what is observed.

[22] What does such a proton (and heavy ion) aurora do to the upper atmosphere and ionosphere? As discussed by *Horanyi et al.* [1988], energetic ion and electron precipitation have similar aeronomical consequences (i.e., they are similar in their overall ionization, heating, emission patterns, etc.) for comparable energy deposition altitudes. Heavy ions of about 100 keV/amu penetrate to roughly the 0.05 μbar level for initial energies of about 100 keV/amu [*Cravens et al.*, 1995]. This depth places most of the energy deposition well above the hydrocarbon layer (or homopause) [*Grodent et al.*, 2001], so that almost all the ultraviolet emission generated by the precipitation escapes from the atmosphere.

[23] *Rego et al.* [1994] explored the effects of auroral proton precipitation at Jupiter and showed that 300 keV protons (almost the same energy as the 200 keV protons in our accelerated solar wind) produce a peak energy deposition at an atmospheric level with a pressure of about 1 μbar. This level is in the vicinity of the homopause so that most of the auroral UV emission would not be absorbed by methane and would be able to escape and be observed. Solar wind proton precipitation should thus produce observable Lyman alpha emission, which should, in fact, be Doppler-shifted and/or broadened by about 1 nm (in wavelength) since the emitting H atoms, from charge transfer, are moving (post acceleration) at about 5000 km/s. Using a rough Lyman alpha efficiency of .003 [*Waite et al.*, 1983], the Lyman α intensity should (very roughly) be 300 kR. Considerable He^+ 30.4 nm emission should also be produced from the charge transfer of accelerated solar wind alpha particles. This helium line emission should be largely absorbed by the molecular hydrogen at higher altitudes.

[24] One difficulty with the above scenario is that both the Birkeland currents and the total auroral power are excessive, and no evidence exists for high-intensity, highly

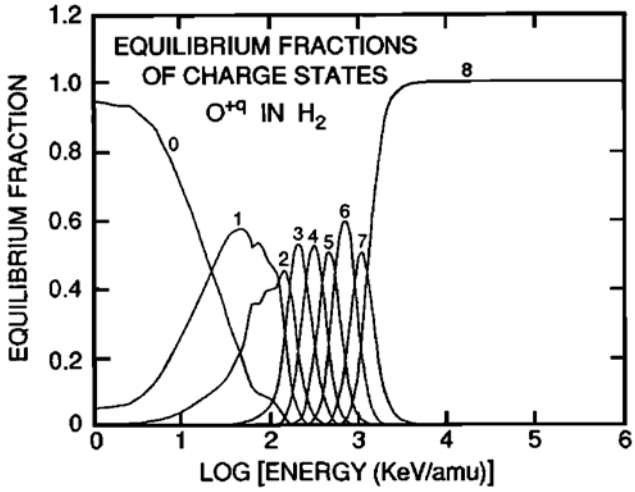

Figure 3. Plot of equilibrium charge fractions for oxygen ions in molecular hydrogen as a function of the base-10 log of the ion energy per amu. From *Cravens et al.* [1995].

Doppler-broadened Lyman alpha emission in the polar cap. In addition, it is difficult to see how the observed 40-min periodicity in the X-ray emission could be generated by solar wind ions precipitating on open magnetic field lines. Nonetheless, some solar wind ion precipitation might occur in the cusp region, although not enough to fully explain the observed X-ray power. An alternate X-ray production scenario is discussed in the next section.

3. X-Ray Emission From Accelerated Outer Magnetospheric Ions

3.1. Ion Populations in the Outer Magnetosphere

[25] In this section of the paper, we assume that ambient ion populations in the outer magnetosphere precipitate into the high-latitude atmosphere and produce X-rays in the form of line emission. The charge states of heavy ions in the Jovian magnetosphere are known to be lower than in the solar wind [*Geiss et al.*, 1992], reflecting their origin in the Io plasma torus (i.e., S^+, S^{++}, S^{+++}, O^+, O^{++}). Such low charge state ions do not produce X-rays when they interact with neutrals, unless they are energetic enough to undergo electron removal (or stripping) collisions with atmospheric target species (i.e., H_2). Figure 3 shows oxygen ion equilibrium fractions (for different charge states and for H_2 targets) as functions of energy [*Cravens et al.*, 1995]. Oxygen ions must have energies in excess of about 1 MeV/amu in order for the charge state to be high enough (i.e., O^{8+} and O^{7+} for oxygen), such that the atomic transitions are in the X-ray part of the spectrum [*Cravens et al.*, 1995; *Kharchenko et al.*, 1998; *Liu and Schultz*, 1999]. Extreme ultraviolet (EUV), rather than X-ray, photons are emitted by O^{5+} ions. Excited O^{5+} ions result from charge transfer collisions of precipitating O^{6+} ions, which are present in oxygen beams with energies of only about 0.5 MeV/amu. Measured ion fluxes at these high energies are quite low in the outer magnetosphere of Jupiter [cf. *Schardt and Goertz*, 1983] and certainly not sufficient to explain the observed X-ray power, even if all the MeV ions observed are interpreted as heavier ions (at least some are protons) and even if the loss cone was fully supplied (neither of which is likely to be the case).

[26] The bulk of the ions observed in the magnetosphere have energies much less than the few MeV we require [cf. *Krimigis and Roelof*, 1983; B. H. Mauk et al., Energetic ion characteristics and gas interactions in Jupiter's magnetosphere, submitted to *Journal of Geophysical Research*, 2003, hereinafter referred to as Mauk et al., submitted manuscript, 2003]. A typical ion density measured in the outer magnetosphere by the Voyager LECP experiment is $n \approx 10^{-3}$ cm^{-3} and a typical temperature is kT $\approx$ 40 keV [*Krimigis and Roelof*, 1983; *Lanzerotti et al.*, 1992; Mauk et al., submitted manuscript, 2003], although densities of $\approx 4 \times 10^{-5}$ cm^{-3} have also been reported from the Ulysses HISCALE experiment [*Desai and Simnett*, 1996; *Hawkins et al.*, 1998]. The proton to heavy ion ratio in the ion fluxes appears to differ considerably for different Ulysses measurements but seems to be somewhere between 1 and 100 [*Desai and Simnett*, 1996]. The Voyager LECP experiment [*Hamilton et al.*, 1981; *Krimigis and Roelof*, 1983] saw the following flux ratios in the outer magnetosphere for comparable energies per charge: H/He $\approx$ 15, He/O $\approx$ 1, and S/O $\approx$ 1. We denote the proton to heavy ion (Z > 2) abundance ratio as $R_{H/O}$ and the helium ion to heavy abundance ratio as $R_{He/O}$. *Krimigis et al.* [1979] concluded that the H and O densities were comparable in the outer magnetosphere with density and temperature as given earlier. Measurements of energetic ions in the magnetosphere made by the Galileo spacecraft showed that at a radial distance of 39 R_J and for energies greater than 50 keV, the proton and oxygen densities are comparable (at $\approx 10^{-3}$ cm^{-3}) and the sulfur density is about 7 time larger (Mauk et al., submitted manuscript, 2003).

[27] The Ulysses HISCALE experiment observed that the energetic ion fluxes (and electron fluxes) showed quasi-periodic behavior, especially at a period of about 40 min [*Anagnostopoulos et al.*, 1998; *Haggerty and Armstrong*, 1999; *Marhavilas et al.*, 2001]. To quote *Marhavilas et al.* [2001], "... a $\approx$ 40 and $\approx$15–20 min periodic variation is a semipermanent characteristic in energetic particle events upstream from the Jovian bow shock, up to distances as far as >1000 R_J" and "..the high latitude magnetosphere seems to play a more important role than the magnetodisk plasma sheet in providing the upstream region with magnetospheric ions".

[28] The charge states of heavy ions in the outer magnetosphere are not well known. A wide range of abundance ratios are quoted in the literature even for the Io plasma torus [e.g., *Bagenal et al.*, 1992; *Geiss et al.*, 1992; *Schreier et al.*, 1998]. In the outer torus (8 or 9 R_J) the abundances of O^+ and O^{++} are apparently roughly comparable, as are the abundances of S^+, S^{++}, and S^{+++}. We will assume for the estimates in this paper that the major ion species is O^{++} (M = 16 amu and q = 2e). The implications of having more singly charged oxygen and the presence of sulfur ions will be considered in the discussion section.

3.2. Acceleration of Magnetospheric Ions by a Parallel Electric Field

[29] The 30 keV or so oxygen or sulfur ions present in the magnetosphere need to be accelerated to energies of

about 1 MeV/amu (or a total energy of $K_{||} \approx M$ MeV, or 16 MeV for oxygen) in order for X-ray emission to occur, and this can be accomplished with a field-aligned potential of $V_{||} \approx K_{||}/q$. For oxygen, with M = 16 and q = 2 (typically), we need a potential of at least $V_{||} \approx 8$ MV, located somewhere along the magnetic field line between the plasma sheet and the top of the atmosphere. Note that if the ions are mainly O^{+} rather than O^{++}, then a potential of about 16 MV is needed instead. This potential will also accelerate sulfur ions, although to somewhat different energies depending on the charge state. The potential will also increase the particle flux into the atmosphere relative to the magnetospheric ion flux at the magnetic equator in the portion of phase space that has access to the acceleration region (i.e., small pitch angles). We estimated this flux from the omnidirectional densities measured near the equator, as discussed above. However, it should be noted that the relevant narrow range of pitch angles is not accessible to spacecraft experiments, so the overall density had to suffice for our estimates. The omnidirectional thermal magnetospheric ion flux is then roughly $F_{th} \approx n\, v_{th} \approx 6 \times 10^{4}$ cm^{-2} s^{-1}, where we adopted a typical density of 10^{-3} cm^{-3} and a thermal speed appropriate for a 40–50 keV thermal energy. Assuming that the mirror ratio is very large, the Knight relation is linear and we have the Knight ratio of $K_{||}/K_{th} \approx 16$ MeV/40–50 keV = 300–400. This ratio gives a particle flux at the top of the atmosphere of $F \approx 400\, F_{th} \approx 2 \times 10^{7}$ cm^{-2} s^{-1}. Next, we consider the X-ray power generated by this particle flux.

[30] The energy input, or power density, for heavy ion precipitation is equal to $F\, K_{||} \approx 16$ MeV $\times\, 2 \times 10^{7}$ cm^{-2} s$^{-1} \approx 0.6$ W m^{-2}. Multiplying this by the area gives the total auroral power for this type of heavy ion precipitation: 6×10^{13} W. The X-ray emission efficiency for heavy ion precipitation at these energies is about $\varepsilon \approx 10^{-3}$ [*Kharchenko et al.*, 1998; *Liu and Schultz*, 1999, 2000], which gives an X-ray luminosity of 60 GW, which is about a factor of 60 more than the observed X-ray power. However, the ion density we adopted for the outer magnetosphere (10^{-3} cm^{-3}) might easily be too large. If the magnetospheric heavy ion density were 3×10^{-5} cm^{-3} rather than 10^{-3} cm^{-3}, as some magnetospheric measurements would support, then the total auroral power from heavy ions would only be $\approx 2 \times 10^{12}$ W (or a energy flux of $\approx$0.01–0.02 W m^{-2}) and the X-ray power would be close to the observed values of 1–2 GW.

[31] The X-ray intensity emitted from the atmosphere can be estimated by multiplying the 0.02 W m^{-2} energy flux (from the preceding paragraph) by the X-ray efficiency and then dividing by a typical X-ray photon energy ($E_{photon} \approx$ 500 eV):

$$4\pi I \approx 0.02\ \mathrm{W\ m^{-2}} \times 10^{-3} \times \left(1.6 \times 10^{-19}\mathrm{J/eV}\right)^{-1}/500\mathrm{eV} \times 10^{-4}\mathrm{m^2/cm^2} \approx 2 \times 10^{7}\mathrm{photons\ cm^{-2}s^{-1}} = 20\ \mathrm{R}. \quad (4)$$

Recall that CXO observed a soft X-ray intensity of roughly 10 R in the polar cap [*Gladstone et al.*, 2002]. The heavy ion flux at the top of the atmosphere for this case is $F \approx 10^{6}$ cm^{-2} s^{-1} and about 10 X-ray photons are produced per incident ion (rather than the 1–3 for the less energetic solar wind ions in the first scenario).

[32] We have produced a reasonable soft X-ray flux using a typical ambient ion population in the outer magnetosphere (to the extent that we know this), but we needed to invoke an 8 million Volt parallel potential. Let us consider some implications of this heavy ion aurora, and the associated proton and alpha particle precipitation. The energy deposition associated with heavy ion precipitation was described by *Horanyi et al.* [1988] and by *Cravens et al.* [1995]. Figure 9 in the work of *Cravens et al.* [1995], which displays energy deposition versus altitude (or density level) for precipitating monoenergetic oxygen ions of different energies, shows that the peak energy deposition for 1 MeV/amu oxygen precipitation takes place at a density level of $\approx 2 \times 10^{12}$ cm^{-3} (or a pressure level of $\approx$0.1 μbar). This pressure level is somewhat above the homopause according to the neutral density profiles shown by *Grodent et al.* [2001]. Lyman and Werner band emission, ionization, and atmospheric heating will be generated by the auroral precipitation.

[33] As just discussed, protons and alpha particles are also present in the outer magnetosphere and will also be accelerated by the 8 MV potential. Proton energies will be about 8 MeV. Helium (i.e., alpha particles) (q = 2 and M = 4) will be accelerated to 16 MeV (that is, 4 MeV/amu). The proton density in the outer magnetosphere is probably about 10–20 times greater than the heavy ion density, in which case the resulting precipitating proton flux is a factor of 5–10 greater than the precipitating heavy ion: $F_{protons} \approx 10^{7}$ cm^{-2} s^{-1}. The associated energy flux is $F_{protons}$ multiplied by 8 MeV, or $\approx$0.1 W m^{-2}, and the total auroral power is $\approx 10^{13}$ W, which is about 10 times less than the total auroral power for the solar wind ions/protons scenario for the same X-ray luminosity. Obviously, adopting a higher proton to heavy ion ratio in the magnetosphere would give a larger total energy flux or power for the same X-ray luminosity. The atmospheric level of the peak energy deposition for 8–16 MeV protons can be roughly estimated by scaling the *Rego et al.* [1994] results using a stopping power that varies roughly as ln(E)/E. The peak energy deposition takes place at a pressure level of $\approx$0.5 mb, which is well below the homopause [*Grodent et al.*, 2001]. Most ultraviolet emissions should not be able to escape from this depth. The small amount of Lyman alpha emission created above the homopause will be highly Doppler-shifted and broadened (about 5 nm). Even though the atmosphere is optically thick to ultraviolet emissions produced deep in the atmosphere at the 0.5 mb level, the considerable auroral heating in the hydrocarbon layer might contribute to the "hot spot" hydrocarbon emissions observed in the polar cap (see the discussion by *Gladstone et al.* [2002]).

[34] The contribution of accelerated helium to the total power will be less than the proton contribution due to the lower helium abundance. Some Doppler-shifted He^{+} 30.4 nm emission will be produced as a consequence of the charge transfer of fast He^{++} ions with atmospheric neutrals, but again the associated energy deposition will occur below the homopause (though not as deep as the proton-associated energy deposition) and almost all of the upwardly traveling photons will surely be absorbed by the overlying atmosphere. A rough estimate of the 30.4 nm

intensity for an equal He to heavy ion ratio ($R_{He/O} \approx 1$) in the outer magnetosphere (neglecting atmospheric absorption) gives ≈100 R.

3.3. Relation Between X-Ray and Total Auroral Power

[35] The total auroral power can be simply related to the X-ray power without explicit reference to the auroral area or to the local emission intensity. As discussed above in a somewhat different context, the total auroral power for heavy ion precipitation (denoted $L_{total/ion}$) is the X-ray luminosity (denoted L_{xray}) divided by the X-ray efficiency ($L_{total/ion} \approx L_{xray}/\varepsilon$). Protons are also accelerated but to energies a factor of 2 less than the total oxygen ion energy (≈8 MeV versus ≈16 MeV). The Knight factor is about a factor of 2 less for protons than for oxygen (due to a smaller $K_{\|}/K_{th}$, assuming equal K_{th} values). Hence the total power in the proton aurora in terms of the x-ray power is just $L_{total/proton} \approx (L_{xray}/\varepsilon)\,(R_{H/O}/4)$. Helium and heavier ions have the same total energy (and the same Knight factor) so that their power contributions differ only by the factor $R_{He/O}$. The total combined (protons, helium, and heavy ions) auroral power (denoted L_{total+}) can be written as:

$$L_{total+} \approx \left(L_{xray}/\varepsilon\right)\left(1 + R_{He/O} + R_{H/O}/4\right)$$

or

$$L_{total+}\left(10^{13}\mathrm{W}\right) \approx 0.1\ L_{xray}(\mathrm{GW})\left(1 + R_{He/O} + R_{H/O}/4\right) \quad (5)$$

L_{total+} (10^{13} W) denotes the auroral power in units of 10^{13} W and L_{xray} (GW) denotes the x-ray luminosity in units of GW. From equation (5), for an x-ray power of 1 GW and for $R_{H/O} = 1$ and $R_{He/O} = 1$, the total auroral power is 2×10^{12} W, whereas for $R_{H/O} = 20$ and $L_{xray} = 1$ GW, the total power is $L_{total+} = 7 \times 10^{12}$ W.

3.4. Birkeland Currents Associated With Ion Precipitation

[36] The Birkeland current associated with the combined proton, helium, and heavy ion fluxes is about 2 MA (1 MA per hemisphere) for a proton to heavy ion ratio of ≈20 and for conditions appropriate for an X-ray power of 1 GW as discussed above. This current can be relatively directly constrained by the observed X-ray power without explicit reference to the magnetospheric ion population, if we assume that the X-rays are produced by heavy S and/or O ions with energies (at the top of the atmosphere) of about 1 MeV/amu or somewhat greater.

[37] The downward Birkeland current (both hemispheres) expressed in terms of the total rate of heavy ions per second impacting the atmosphere (call this Q) is given by the expression:

$$I_{\|+} \approx Qe\left[\langle q\rangle + 2R_{He/O} + 0.5R_{H/O}\right], \quad (6)$$

where e is the electron charge and $\langle q\rangle$ is the average charge on a heavy ion ($Z > 2$) in the magnetosphere. The factor of 2 in front of $R_{He/O}$ is due to the charge on He^{++} and the factor of 0.5 in front of $R_{H/O}$ is due to a smaller Knight factor for protons than for O^{++} ions. The heavy ion impact rate, Q, can be related to the observed total auroral x-ray power/luminosity (denoted L_{xray}) with the expression:

$$Q \approx L_{xray}/\left[\varepsilon\ K_{\|}\right], \quad (7)$$

where ε and $K_{\|}$ are the x-ray efficiency ($\approx 10^{-3}$) and the impact energy ($K_{\|} \approx 16$ MeV), respectively. Equations (6) and (7) together can be rewritten as:

$$I_{\|+} \approx 0.1\ \mathrm{MA}\ L_{xray}(\mathrm{GW})\left[\langle q\rangle + 2R_{He/O} + 0.5R_{H/O}\right]. \quad (8)$$

In the brackets of equation (8), the first term is due to the heavy ion current, the second term is due to the alpha particle current, and the third term is due to the proton current. For $R_{H/O} = 20$, $R_{He/O} = 1$, $\langle q\rangle = 2$ and $L_{xray} = 1$ GW, then $I_{\|+} \approx 1-2$ MA.

[38] An expression like equation (6) can be written for the SWCX mechanism but without the 0.5 in front of $R_{H/O}$ (a factor 2 appears instead due to the Knight factor) and with $\langle q\rangle \approx 7$ for the solar wind. For the SWCX mechanism, the total number of solar wind heavy ions impacting the atmosphere can be expressed in terms of the X-ray luminosity and the photon energy (about 300–500 eV) and the number of X-ray photons per excited heavy ion (2 is assumed): $Q_{sw/h} \approx L_{xray}/[2\ E_{photon}]$. This current can be written as:

$$I_{\|+} \approx Q_{sw/h}e\left[\langle q\rangle + 2R_{He/O} + 2R_{H/O}\right]. \quad (9)$$

The factor $R_{H/O}$ is also equal to 1/f. Equation (9) gives currents of about 1–3 GW when the observed x-ray luminosity is used.

4. Electron Contributions to Birkeland Currents

[39] Precipitating energetic charged particles, whether electrons or ions, ionize neutrals in the atmosphere, thus producing secondary electrons. The secondary electrons have a wide range of energies but the average energy is about 50 eV, roughly independent of the incident energy [cf. *Waite et al.*, 1983; *Horanyi et al.*, 1988]. In this section, the Birkeland current carried by the secondary electrons is discussed after a brief initial discussion of electron precipitation in the main auroral oval.

4.1. Main Auroral Oval – Electron Precipitation

[40] We now estimate the total (upward) Birkeland current associated with the main auroral oval at Jupiter, as discussed in the introduction. This current can be related to the total auroral power associated with the precipitating energetic electrons thought to be responsible for the main oval. In terms of the average energy of an incident electron at the top of the atmosphere (E_0) and the total auroral power for the main oval ($L_{tot/e}$), the total rate of electron entry into the atmosphere is $Q_e = L_{tot/e}/E_0$. This total auroral power has been deduced from the observed auroral ultraviolet intensities (mainly in the Lyman and Werner band systems of molecular hydrogen) plus reasonable emission efficiencies (see the reference list in the work of *Bhardwaj and Gladstone* [2000]). The associated upward total Birkeland current is then $I_{\|e} = Q_e\ e$, which is independent of the area

of precipitation or of the local intensity of precipitation. This current can be written as:

$$I_{\|e} = e\, L_{tot/e}/E_0$$

or

$$I_{\|e} = 10^4 MA\ L_{tot/e}(10^{13}W)/E_0(keV). \qquad (10')$$

For example, for a 10^{13} W aurora and for 100 keV electrons, the current (both hemispheres) is 100 MA, which is in line with the current estimates of *Bunce and Cowley* [2001] and *Cowley et al.* [2003]. Precipitating electrons produce secondary electrons, some of which will escape from the atmosphere; however, the field-aligned potential which accelerates the primary electrons reflects these lower energy secondary electrons back to the planet so that they do not make a contribution to the net Birkeland current.

4.2. Secondary Electron Contribution to Birkeland Currents for Heavy Ion and Proton Precipitation

[41] Now we return to the discussion of ion precipitation. Any electrons moving upward from the atmosphere, including secondary electrons, which encounter the field-aligned potential region will be accelerated to energies (for the scenario discussed in this paper) of ≈8 MeV. A consequence of this acceleration will be the presence of beamlike counterstreaming (both hemispheres contribute) electrons in the outer magnetosphere. These electrons also carry a downward Birkeland current into the ionosphere. The potential drop region is likely to be at least several Jovian radii above the surface because the mirror ratio needs to be about 200–400. The question that needs to be answered in this section is what is the flux of electrons escaping the atmosphere/ionosphere and thus reaching this acceleration region?

[42] The ionospheric thermal plasma has a scale height of a few hundred kilometers [cf. *Waite and Cravens*, 1987] so that the density (or flux) of "thermal" electrons at a radial distance of a few R_J (where the potential is likely to be located) is extremely small. The flux of photoelectrons produced by the photoionization of atmospheric neutrals by solar radiation will also be very small in the high-latitude auroral region.

[43] Now consider what happens to the secondary electrons produced by the (primary) auroral ion precipitation. These electrons are produced by ionization and stripping processes [*Cravens et al.*, 1995]. Unfortunately, a fully relevant calculation of the secondary electron escape flux for heavy ion and proton precipitation has not been undertaken, although some information can be found in the work of *Horanyi et al.* [1988] or *Cravens et al.* [1995]. Using the secondary electron flux at 450 km due to oxygen precipitation calculated by Horanyi et al., we estimate the average secondary electron energy to be $\langle E \rangle \approx 10-50$ eV. Beyond an altitude of a few thousand km, secondary electrons should be the dominant electron population, and they will determine the upward polarization electric field [cf. *Cravens*, 1997b]. The associated polarization potential drop is roughly equal to the average electron energy divided by the electron charge. This polarization field reflects electrons with energies less than about the average energy $\langle E \rangle$. Adopting $\langle E \rangle \approx 25$ eV for this average energy, we estimate an electron escape flux of $F_{sec} \approx 10^8$ cm^{-2} s^{-1} for the auroral heavy ion energy flux of 100 ergs cm^{-2} s^{-1} (that is, 0.1 W m^{-2}) used by Horanyi et al. or an electron flux of $\approx 2 \times 10^7$ cm^{-2} s^{-1} for the primary ion flux needed to get a 1 GW X-ray power in the current paper's scenario. It should be emphasized that this electron flux is a very rough estimate and a careful calculation needs to be undertaken.

[44] The escaping electrons reach the large parallel potential region at several R_J and are accelerated outward to energies of about 8 MeV or greater. These electrons carry a downward Birkeland current which we estimate as the escape flux of electrons multiplied by the electron charge and the auroral area. Normalizing this current to the X-ray luminosity gives:

$$I_{\|sec/i} \approx 6\ MA\ L_{xray}(GW). \qquad (10'')$$

The contributions of the secondary electrons from the proton and He^{++} precipitation are omitted from equation (10) because the energy deposition (including impact ionization) takes place so deep in the atmosphere that it is unlikely that many electrons will be able to escape upward. However, this statement really needs to be backed up with careful calculations. The current from secondary electrons for a 1 GW X-ray ion aurora is about 6 MA (with great uncertainty) according to equation (10), and the total ion current (from equation (8), this is somewhat more certain) is about 1–2 MA, giving a total Birkeland current of about 8 MA.

5. Discussion

[45] Two scenarios for auroral soft X-ray emission at Jupiter were presented in this paper. For the first scenario, highly charged solar wind heavy ions precipitate into the atmosphere along cusp/cleft magnetic field lines and produce X-rays due to charge transfer collisions. Additional acceleration of these ions by a ≈200 kV field-aligned potential is required to generate the observed X-ray power of about 1 GW. For the second scenario, heavy ions (mainly oxygen and sulfur) residing in the outer magnetosphere are accelerated by a field-aligned potential of about 8 MV or greater and precipitate into the atmosphere where high charge state ions are created by electron removal collisions. These ions then emit X-rays when they undergo charge transfer collisions or direct excitation collisions with atmospheric target gases. The potential is needed to boost the originally low charge state ions to energies high enough for high charge states to be created when the ions precipitate into the auroral atmosphere. Note that if the magnetospheric ions are O^+ rather than O^{++}, then the potential needs to be in excess of 16 MV and the specific numbers estimated throughout the paper will change somewhat. In this case, the precipitating protons would be accelerated to 16 MeV and the outwardly accelerated electrons would also have energies of 16 MeV.

[46] Observations of auroral hiss at Jupiter made by the Ulysses radio experiment [*Farrell et al.*, 2003] suggest that perhaps a solar wind power of $10^{10}-10^{12}$ W into the cusp. Roughly applying a heavy ions fraction of 10^{-3} and an X-ray efficiency of 0.1% gives an X-ray power of less than 1 MW without acceleration and less than 100 MW with

acceleration, thus agreeing with other evidence that a pure solar wind explanation for the Jovian X-ray aurora is not likely.

5.1. Proton Aurora

[47] In both scenarios, protons and alpha particles, as well as heavy ions, are accelerated and precipitate into the atmosphere. In both cases, the proton component accounts for most of the total auroral power as well as producing Lyman alpha emission. In fact, the relative proton abundance in the solar wind is sufficiently high that the predicted total auroral power in the polar cap ($\approx 10^{14}$ W) and the estimated Lyman alpha intensity (about 300 kR) are probably excessive enough to exclude a pure solar wind scenario. In the magnetospheric scenario the protons are quite energetic (8–16 MeV) and precipitate down to altitudes well below the homopause (that is, deep into the hydrocarbon layer) where they might account for the high-latitude hydrocarbon "hotspot" observed in the infrared part of the spectrum (see the discussion by *Bhardwaj and Gladstone* [2000] or by *Gladstone et al.* [2002]).

5.2. Birkeland Currents

[48] Significant Birkeland currents are associated with both X-ray aurora scenarios. For the magnetospheric ion scenario, these downward currents represent part of the "return current" of the magnetosphere-ionosphere circuit discussed by *Hill* [2001], *Bunce and Cowley* [2001], and other workers (see the discussion by *Cowley et al.* [2003]). The upward current part of the circuit attaches to the main auroral oval (radial distance of about 30 R_J) and is carried by precipitating electrons. If indeed precipitating magnetospheric heavy ions are responsible for the X-ray aurora at Jupiter, then the observed X-ray emission (and images) is mapping out return current in the polar cap region (with estimated currents of $\approx$8 MA associated with the X-ray emission), just as main auroral oval emissions map out the upward current portion of the circuit. In this case, observations of Jovian X-ray emission puts constraints on the magnetospheric dynamics at Jupiter.

[49] Currents of about 1000 MA were estimated for the accelerated solar wind scenario due to the high solar wind proton abundance relative to heavy ions. The current system for this case must involve the magnetosheath plasma in the vicinity of the cusp part of the magnetopause. These very high current estimates suggest that a pure solar wind X-ray production scenario is unlikely.

5.3. X-Ray Spectrum

[50] The rather low resolution ROSAT/PSPC spectrum shown by *Waite et al.* [1994] appears to agree with a line-emitting energetic ion aurora scenario [e.g., *Cravens et al.*, 1995], but the model-observation comparisons were not conclusive. We are currently awaiting the analysis of higher resolution spectra of the Jovian aurora made by the CXO ACIS instrument in February 2003. These spectra will hopefully provide clues on the source of the X-ray emission. If the spectra indicate the presence of transitions from highly charged sulfur and oxygen ions, then this would favor the magnetospheric ion scenario. Identification of individual lines (or groups of lines) for specific charge states could then be used, together with charge state equilibrium fractions (such as those shown in Figure 3), to deduce the energy of the incident auroral ion beam (and hence the value of the accelerating potential). Note that an 8 MV potential, which accelerates O^{++} ions to $\approx$1 MeV/amu (at which energy oxygen is fully stripped upon entering the Jovian atmosphere) will accelerate S^{++} ions to an energy of 0.5 MeV/amu, leaving these ions with a considerable number of remaining electrons. Each ion charge state will emit a characteristic set of lines which allows the charge state composition to be extracted from a sufficiently high resolution auroral X-ray spectrum.

5.4. Periodicity in the X-Ray Emission

[51] One of the more surprising features of the x-ray aurora observed by CXO [*Gladstone et al.*, 2002] was a strong 40-min periodicity. As mentioned in the introduction, similar periodicities appear in measured energetic electron and ion populations and in Jovian radio emission. *MacDowall et al.* [1993] reported on Ulysses URAP (Unified Radio and Plasma Wave Experiment) measurement of quasi-periodic radio bursts in the 1–200 kHz range which displayed 40 min (or so) periodicity (QP-40 bursts) and which were associated with keV and MeV electron bursts of similar periodicity. The QP-40 bursts seen by Ulysses were apparently produced from a source region located about 5 R_J above the south pole (Figure 8 in the work of *MacDowall et al.* [1993]). A likely mechanism for this radio emission is the electron cyclotron maser instability which requires the existence of accelerated electrons. The linkage of the radio emission to the periodic X-ray emission can perhaps be provided by the upward acceleration of secondary electrons discussed in this paper (to energies of $\approx$8–16 MeV for the magnetospheric ion case). The few R_J location of the acceleration region deduced from the radio emission is consistent with the mirror ratio arguments made earlier in the paper. MacDowall et al. also demonstrated that the probability of detecting QP-40 bursts was correlated with solar wind velocity.

[52] Impulsive bursts of relativistic electrons were observed on the outbound leg of Ulysses' encounter with Jupiter (i.e., high-latitude southern hemisphere dusk magnetosphere), and the electron fluxes exhibited 40 min periodicities [*Simpson et al.*, 1992; *McKibben et al.*, 1993]. Furthermore, the radio onsets seem to precede the electron bursts observed at Ulysses by a few minutes, and the pitch-angle characteristics of the electrons suggest that they are (according to *McKibben et al.* [1993]) "streaming outwards along field lines that connect to Jupiter at high southern latitude." These observational characteristics seem to support our explanation of outwardly streaming secondary electrons accelerated by a field-aligned potential at distances from Jupiter of several R_J. Note that an escape flux of electrons of $\approx 2 \times 10^7$ cm^{-2} s^{-1}, which we estimated earlier, will become a field-aligned flux of $\approx$200 cm^{-2} s^{-1} at a distance of 50 R_J (estimated with a field strength that varies with distance like a dipole), whereas the observed flux of electrons with energies in excess of 8–16 MeV is not too different at a value of about 300 cm^{-2} s^{-1} according to *McKibben et al.* [1993]. A search by the Galileo EPD did not detect MeV electron beams at radial distances of 39 R_J and 46 R_J [*Williams et al.*, 1996]; however, due to data rate limitations, a comprehensive survey was not undertaken, and the acceleration region

could easily be located on field lines whose equatorial distance exceeds 46 R_J.

[53] The 40 min periodicities observed in X-rays, energetic particles, and radio emission are all linked, which makes sense given the discussion in this paper, but we are still missing an explanation for why a periodicity is associated with any of these phenomena. If the explanation involves some "bounce" type periodicity in particle motion or some MHD standing wave pulsation, then the magnetospheric X-ray scenario (which takes place on closed field lines) would be more likely than a pure solar wind scenario. *Desch* [1994] suggested that this phenomenon might be similar to terrestrial substorms.

6. Conclusions

[54] This paper has explored two scenarios in which energetic ion precipitation produces the observed Jovian auroral X-ray emission from high latitudes. In one case, high charge state solar wind heavy ions are accelerated to about 200 keV, which boosts their flux and produce X-rays in charge transfer collisions with neutrals. In the second case, heavy Jovian ions residing in the outer magnetosphere (e.g., sulfur and oxygen) are accelerated to energies in excess of 8 MeV. This acceleration not only boosts the ion flux but also increases the charge state of the ions as they collide with the atmosphere. These ions produce X-rays as a by-product of charge transfer or direct excitation collisions. The magnetospheric ion scenario seems more likely for a number of reasons which were discussed in the paper. The downward Birkeland current carried by the ions and by upward moving accelerated electrons for the second case is about 8 MA. The auroral X-ray emission is a diagnostic of at least some of the return current in the equivalent magnetospheric electrical circuit. The specific atomic lines present in measured high-resolution X-ray spectra of the aurora will point to the specific charge states of the emitting ion species, which can then be used as a diagnostic of the ion energy (and thus of the parallel potential drop). The field-aligned potential is created due to "excessive" current demands of the magnetospheric circuit (see *Mauk et al.* [2002] or *Cowley et al.* [2003] and references in these papers). High-resolution X-ray spectra will also be able to distinguish between the solar scenario and the magnetospheric ion scenario due to the different spectral signatures of the different species (e.g., more carbon in the solar wind spectrum) and charge states for the two scenarios. Finally, the outwardly moving secondary electrons, which are accelerated to energies exceeding 8 MeV, could be responsible for some of the energetic electrons observed in the magnetosphere as well as for some observed radio emissions, both of which have 40 min periodicities, just like the X-ray emission.

[55] **Acknowledgments.** We acknowledge support from NASA Planetary Atmospheres grant NAG5-11038.

[56] Arthur Richmond thanks Stanley Cowley and Vasili Kharchenko for their assistance in evaluating this paper.

References

Anagnostopoulos, G. C., P. K. Marhavilas, E. T. Sarris, I. Karanikola, and A. Balogh, Energetic ion populations and periodicities near Jupiter, *J. Geophys. Res.*, *103*, 20,055, 1998.

Bagenal, F. D., E. Shemansky, R. L. McNutt Jr., R. Schreir, and A. Eviatar, The abundance of O^{++} in the Jovian magnetosphere, *Geophys. Res. Lett.*, *19*, 79, 1992.

Barbosa, D. D., Dynamics of field-aligned current sources at Earth and Jupiter, in *Magnetospheric Currents*, *Geophys. Monogr. Ser.*, vol. 28, edited by T. A. Potemra, p. 350, AGU, Washington, D. C., 1984.

Barbosa, D. D., Heavy ion dynamics and auroral arc formation in the Jovian magnetosphere, *Adv. Space Res.*, *12*, 7, 1992.

Bhardwaj, A., and G. R. Gladstone, Auroral emissions of the giant planets, *Rev. Geophys.*, *38*, 395, 2000.

Bunce, E. J., and S. W. H. Cowley, Divergence of the equatorial current in the dawn sector of Jupiter's magnetosphere: Analysis of Pioneer and Voyager magnetic data, *Planet. Space Sci.*, *49*, 1089, 2001.

Bunce, E. J., P. G. Hanlon, and S. W. H. Cowley, A simple empirical model of the equatorial radial field in Jupiter's middle magnetosphere based on fly-by and Galileo orbiter data, *Planet. Space Sci.*, *50*, 789, 2002.

Clarke, J. T., et al., Hubble Space Telescope imaging of Jupiter's UV aurora during the Galileo orbiter mission, *J. Geophys. Res.*, *103*, 20,217, 1998.

Cowley, S. W. H., and E. J. Bunce, Origin of the main auroral oval in Jupiter's coupled magnetosphere-ionosphere system, *Planet. Space Sci.*, *49*, 1067, 2001.

Cowley, S. W. H., A. Balogh, M. K. Dougherty, M. W. Dunlop, T. M. Edwards, R. J. Forsyth, N. F. Laxton, and K. Staines, Plasma flow in the jovian magnetosphere and related magnetic effects: Ulysses observations, *J. Geophys. Res.*, *101*, 15,197, 1996.

Cowley, S. W. H., E. J. Bunce, and J. D. Nichols, Origins of Jupiter's main oval auroral emissions, *J. Geophys. Res.*, *108*(AX), 8002, doi:10.1029/2003JA009329, 2003.

Cravens, T. E., Comet Hyakutake x-ray source: Charge transfer of solar wind heavy ions, *Geophys. Res. Lett.*, *24*, 105, 1997a.

Cravens, T. E., *Physics of Solar System Plasmas*, Cambridge Univ. Press, New York, 1997b.

Cravens, T. E., X-ray emission from comets, *Science*, *296*, 1042, 2002.

Cravens, T. E., and A. N. Maurellis, X-ray emission from scattering and fluorescence of solar x-rays at Venus and Mars, *Geophys. Res. Lett.*, *28*, 3043, 2001.

Cravens, T. E., E. Howell, J. H. Waite Jr., and G. R. Gladstone, Auroral oxygen precipitation at Jupiter, *J. Geophys. Res.*, *100*, 17,153, 1995.

Desai, M. I., and G. M. Simnett, Solar wind driven flows in the Jovian magnetosphere, *J. Geophys. Res.*, *101*, 13,115, 1996.

Desch, M. D., Jupiter radio bursts and particle acceleration, IAU Symposium in Particle Acceleration, *Astrophys. J. Suppl. Ser.*, *90*, 541, 1994.

Dougherty, M. K., D. J. Southwood, A. Balogh, and E. J. Smith, Field-aligned currents in the Jovian magnetosphere during the Ulysses flyby, *Planet. Space Sci.*, *41*, 291, 1993.

Engle, I. M., and D. B. Beard, Idealized Jovian magnetosphere shape and field, *J. Geophys. Res.*, *85*, 579, 1980.

Farrell, W. M., et al., Ulysses observations of auroral hiss at high Jovian latitudes, *Geophys. Res. Lett.*, *98*, 2259, 1993.

Galand, M., and S. Chakrabarti, Auroral processes in the solar system, in *Atmospheres in the Solar System*: *Comparative Aeronomy*, *Geophys. Monogr. Ser.*, vol. 130, edited by M. Mendillo, A. Nagy, and J. H. Waite, p. 55, AGU, Washington, D. C., 2002.

Gehrels, N., and E. C. Stone, Energetic oxygen and sulfur ions in the Jovian magnetosphere and their contribution to the auroral excitation, *J. Geophys. Res.*, *88*, 5537, 1983.

Geiss, J., et al., Plasma composition in Jupiter's magnetosphere, Initial results from the solar wind ion composition spectrometer, *Science*, *257*, 1535, 1992.

Gérard, J.-C., V. Dols, F. Paresce, and R. Prangé, Morphology and time variation of the Jovian far UV aurora: Hubble Space Telescope observations, *J. Geophys. Res.*, *98*, 18,793, 1993.

Gérard, J.-C., V. Dols, F. Paresce, and R. Prangé, The morphology of the north jovian ultraviolet aurora observed with the Hubble Space Telescope, *Planet. Space Sci.*, *42*, 905, 1994.

Gladstone, G. R., et al., A pulsating auroral x-ray hot spot on Jupiter, *Nature*, *415*, 1000, 2002.

Greenwood, J. B., I. D. Williams, S. J. Smith, and A. Chutjian, Experimental investigation of the processes determining x-ray emission intensities from charge-exchange collisions, *Phys. Rev. A*, *63*, 62,707, 2001.

Grodent, D., J. H. Waite, and J. C. Gerard, A self-consistent model of the Jovian auroral thermal structure, *J. Geophys. Res.*, *106*, 12,933, 2001.

Haggerty, D., and T. P. Armstrong, Observations of Jovian upstream events by Ulysses, *J. Geophys. Res.*, *104*, 4629, 1999.

Hamilton, D. C., G. Gloeckler, S. M. Krimigis, and L. J. Lanzerotti, Composition of nonthermal ions in the Jovian magnetosphere, *J. Geophys. Res.*, *86*, 8301, 1981.

Hawkins, S., III, A. F. Cheng, and L. J. Lanzerotti, Bulk flows of hot plasma in the Jovian magnetosphere: A model of anisotropic fluxes of energetic ions, *J. Geophys. Res.*, *103*, 20,031, 1998.

Hill, T. W., Inertial limit on corotation, *J. Geophys. Res.*, *84*, 6554, 1979.
Hill, T. W., The Jovian auroral oval, *J. Geophys. Res.*, *106*, 8101, 2001.
Horanyi, M., T. E. Cravens, and J. H. Waite Jr., The precipitation of energetic heavy ions into the upper atmosphere of Jupiter, *J. Geophys. Res.*, *93*, 7251, 1988.
Kharchenko, V., W. Liu, and A. Dalgarno, X-ray and EUV emission spectra of oxygen ions precipitating into the Jovian atmosphere, *J. Geophys. Res.*, *103*, 26,687, 1998.
Khurana, K. K., Influence of solar wind on Jupiter's magnetosphere deduced from currents in the equatorial plane, *J. Geophys. Res.*, *106*, 25,999, 2001.
Knight, S., Parallel electric fields, *Planet. Space Sci.*, *21*, 741, 1973.
Krasnopolsky, V. A., et al., X-ray emission from comet McNaught-Hartley (C/1999 T1), *Icarus*, *160*, 437, 2002.
Krimigis, S. M., and E. C. Roelof, Low-energy particle population, in *Physics of the Jovian Magnetosphere*, *Cambridge Planet. Sci. Ser.*, edited by A. J. Dessler, pp. 106–156, Cambridge Univ. Press, New York, 1983.
Krimigis, S. M., et al., Hot plasma environment at Jupiter: Voyager 2 results, *Science*, *206*, 977, 1979.
Lanzerotti, L. J., et al., The hot plasma environment at Jupiter: Ulysses results, *Science*, *257*, 1518, 1992.
Lisse, C. M., et al., Discovery of x-ray and extreme ultraviolet emission from Comet C/Hyakutake 1996B2, *Science*, *274*, 205, 1996.
Lisse, C. M., et al., Charge exchange-induced X-ray emission from Comet C/1999 S4 (LINEAR), *Science*, *292*, 1343, 2001.
Liu, W., and D. R. Schultz, Jovian x-ray aurora and energetic oxygen ion precipitation, *Astrophys. J.*, *526*, 538, 1999.
Liu, W., and D. R. Schultz, Ultraviolet emission from oxygen precipitating into the Jovian aurora, *Astrophys. J.*, *530*, 500, 2000.
Lyons, L. R., The field-aligned current versus electric potential relation and auroral electrodynamics, in *Physics of Auroral Arc Formation*, *Geophys. Monogr. Ser.*, vol. 25, p. 252, AGU, Washington, D. C., 1982.
MacDowall, R. J., M. J. Kaiser, M. D. Desch, W. M. Farrell, R. A. Hess, and R. G. Stone, Quasiperiodic Jovian radio bursts: Observations from the Ulysses Radio and Plasma Wave Experiment, *Planet. Space Sci.*, *41*, 1059, 1993.
Marhavilas, P. K., G. C. Anagnostopoulos, and E. T. Sarris, Periodic signals in Ulysses' energetic particle events upstream and downstream from the Jovian bow shock, *Planet. Space Sci.*, *49*, 1031, 2001.
Mauk, B. H., B. J. Anderson, and R. M. Thorne, Magnetosphere-ionosphere coupling at Earth, Jupiter, and Beyond, in *Atmospheres in the Solar System*: *Comparative Aeronomy*, *Geophys. Monogr. Ser.*, vol. 130, edited by M. Mendillo, A. Nagy, and J. H. Waite, p. 115, AGU, Washington, D. C., 2002.
Maurellis, A. N., T. E. Cravens, G. R. Gladstone, J. H. Waite, and L. W. Acton, Jovian x-ray emission from solar x-ray scattering, *Geophys. Res. Lett.*, *27*, 1339, 2000.
McKibben, R. B., J. A. Simpson, and M. Zhang, Impulsive bursts of relativistic electrons discovered during Ulysses' traversal of Jupiter's dusk-side magnetosphere, *Planet. Space Sci.*, *41*, 1041, 1993.
Metzger, A. E., D. A. Gilman, J. L. Luthey, K. C. Hurley, H. W. Schnopper, F. D. Seward, and J. D. Sullivan, The detection of X-rays from Jupiter, *J. Geophys. Res.*, *88*, 7731, 1983.
Onsager, T. G., C. A. Kletzing, J. B. Austin, and H. MacKiernan, Model of magnetosheath plasma in the magnetosphere: Cusp and mantle particles at low-altitudes, *Geophys. Res. Lett.*, *20*, 479, 1993.
Prangé, R., et al., Detailed study of FUV Jovian auroral features with the post-COSTAR HST faint object camera, *J. Geophys. Res.*, *103*, 20,195, 1998.
Rego, D., R. Prangé, and J.-C. Gérard, Auroral Lyman α and H2 bands from the giant planets: 1. Excitation by proton precipitation in the Jovian atmosphere, *J. Geophys. Res.*, *99*, 17,075, 1994.
Reiff, P. H., T. W. Hill, and J. L. Burch, Solar wind plasma injection at the dayside magnetospheric cusp, *J. Geophys. Res.*, *82*, 479, 1977.
Schardt, A. W., and C. K. Goertz, High-energy particles, in *Physics of the Jovian Magnetosphere*, *Cambridge Planet. Sci. Ser.*, edited by A. J. Dessler, p. 157, Cambridge Univ. Press, New York, 1983.
Schreier, R., A. Eviatar, and V. M. Vasyliunas, A two-dimensional model of plasma transport and chemistry in the Jovian magnetosphere, *J. Geophys. Res.*, *103*, 19,901, 1998.
Simpson, J. A., et al., Energetic charged-particle phenomena in the Jovian magnetosphere: First results from the Ulysses COSPIN collaboration, *Science*, *257*, 1543, 1992.
Vasyliunas, V. M., Plasma distribution and flow, in *Physics of the Jovian Magnetosphere*, edited by A. J. Dessler, chap. 11, p. 395, Cambridge Univ. Press, New York, 1983.
Waite, J. H., Jr., and T. E. Cravens, Current review of the Jupiter, Saturn, and Uranus ionospheres, *Adv. Space Sci.*, *7*(12), 119, 1987.
Waite, J. H., and D. Lummerzheim, Comparison of auroral processes: Earth and Jupiter, in *Atmospheres in the Solar System: Comparative Aeronomy*, *Geophys. Monogr. Ser.*, vol. 130, edited by M. Mendillo, A. Nagy, and J. H. Waite, p. 115, AGU, Washington, D. C., 2002.
Waite, J. H., Jr., T. E. Cravens, J. U. Kozyra, A. F. Nagy, S. K. Atreya, and R. H. Chen, Electron precipitation and related aeronomy of the Jovian thermosphere and ionosphere, *J. Geophys. Res.*, *88*, 6143, 1983.
Waite, J. H., et al., Jovian bremsstrahlung x-rays: A Ulysses prediction, *Geophys. Res. Lett.*, *19*, 83, 1992.
Waite, J. H., Jr., F. Bagenal, F. Seward, C. Na, G. R. Gladstone, T. E. Cravens, K. C. Hurley, J. T. Clarke, R. Elsner, and S. A. Stern, ROSAT observations of the Jupiter aurora, *J. Geophys. Res.*, *99*, 14,799, 1994.
Waite, J. H., Jr., et al., An auroral flare at Jupiter, *Nature*, *410*, 787, 2001.
Walt, M., *Introduction to Geomagnetically Trapped Radiation*, Cambridge Univ. Press, New York, 1994.
Williams, D. J., B. Mauk, R. W. McEntire, E. C. Roelof, T. P. Armstrong, B. Wilken, J. G. Roederer, S. M. Krimigis, T. A. Fritz, and L. J. Lanzerotti, Electron beams and ion composition measured at Io and in its torus, *Science*, *274*, 401, 1996.

T. E. Cravens, Department of Physics and Astronomy, University of Kansas, Lawrence, KS 66045, USA. (cravens@ukans.edu)

G. R. Gladstone, Department of Space Science, Southwest Research Institute, 6220 Culebra Road, P.O. Drawer 28510, San Antonio, TX 78228, USA. (randy.gladstone@swri.org)

T. I. Gombosi, N. Lugaz, and J. H. Waite, AOSS Department, Space Physics Research Laboratory, University of Michigan, 2455 Hayward, Ann Arbor, MI 48109, USA. (tamas@umich.edu; nlugaz@umich.edu; hunterw@umich.edu)

R. J. MacDowall, NASA Goddard Space Flight Center, Mail Code 695, Greenbelt, MD 20771, USA. (robert.j.macdowall@nasa.gov)

B. H. Mauk, Applied Physics Laboratory, Johns Hopkins University, Laurel, MD 20723, USA. (barry.mauk@jhuapl.edu)